Title
THERMOSIPHON WATER HEATERS WITH HEAT EXCHANGERS

Author
Mertol, Atila

Publication Date
1980-06-01

Lawrence Berkeley Laboratory
UNIVERSITY OF CALIFORNIA

ENERGY & ENVIRONMENT DIVISION

Presented at the American Section/International Solar Energy Society Solar Jubilee, Phoenix, AZ, June 2-6, 1980

THERMOSIPHON WATER HEATERS WITH HEAT EXCHANGERS

Atila Mertol, Wayne Place, Tom Webster, and Ralph Greif

June 1980

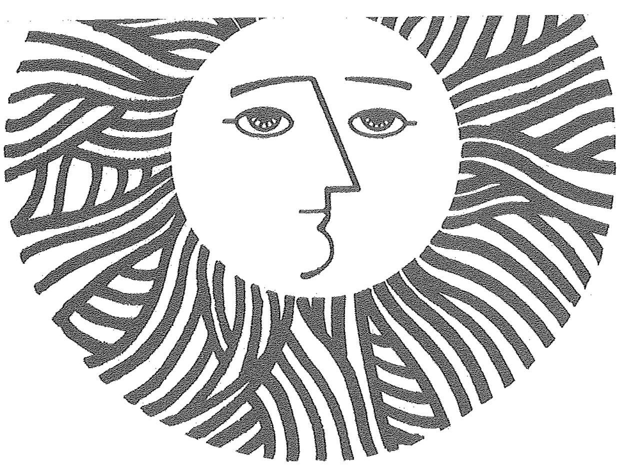

Prepared for the U.S. Department of Energy under Contract W-7405-ENG-48

DISCLAIMER

LBL-10033
June 1980

THERMOSIPHON WATER HEATERS WITH HEAT EXCHANGERS*

A. Mertol, W. Place and T. Webster
Passive Solar Analysis and Design Group
Lawrence Berkeley Laboratory
Berkeley, California 94720

R. Greif
Department of Mechanical Engineering
University of California
Berkeley, California 94720

ABSTRACT

An analytical Detailed Loop Model (DLM) has been developed to analyze the performance of solar thermosiphon water heaters with heat exchangers in storage tanks. The model has been used to study performance of thermosiphons as a function of heat exchanger characteristics, heat transfer fluids, flow resistances, tank stratification, and tank elevation relative to the collector. The results indicate that reasonable performance can be attained with these systems compared to thermosiphons without heat exchangers.

INTRODUCTION

Thermosiphon systems for domestic water heating have been used in various parts of the world for many years and have shown performance comparable to active (pumped) systems [1-3]. However, current work in the United States continues to focus on the development of active systems. This emphasis is attributable in part to the vulnerability of conventional thermosiphons to freezing of water in the low-mass collectors. Studies of more freeze-resistant, high-mass systems, such as "compact heaters," have shown that the performance of the systems is significantly reduced if movable insulation is not used at night [4]. One method of providing freeze protection for thermosiphons with low-mass collectors is the use of a non-freezing heat transfer fluid circulating in a loop consisting of the collector, connecting pipes, and a heat exchanger inside the water storage tank (cf. Fig. 1).

In this work, an analytical Detailed Loop Model (DLM) has been developed to study both daytime and nighttime behavior of such a system. A propylene-glycol (p-glycol) solution (60% by weight) has been selected for the heat transfer fluid because of its low freezing point, low toxicity, and familiarity to the solar industry. Recent trends indicate that p-glycol will be accepted for use with single wall heat exchangers [5].

The basic conservation equations of the system are averaged over the cross-section so that the only space coordinate is "s," which varies along the thermosiphon loop [6]. The flow is assumed to be laminar and the density of the circulating fluid is taken to be constant, except in the buoyancy term, where it is assumed to vary linearly with temperature (Boussinesq approximation). The viscosity of the circulating fluid is evaluated at the average temperature of each system component in accordance with the temperature dependence indicated in Fig. 2. The average temperature of the storage water is determined at each time step by performing an energy balance on the tank. The storage water temperature is assumed to vary linearly with the vertical position in the tank. Other basic assumptions include the following:

- Negligible collector capacitance and incident angle effects.
- Collector parameters based on actual data for a typical one-cover, selective surface collector.
- Constant overall heat transfer coefficients for the collector and heat exchanger (U_c and U_{he}).
- Design day data based on the monthly aver-

*This work was supported by the Passive and Hybrid Systems Branch, Systems Development Division, Office of Solar Applications, U.S. Department of Energy, under contract No. W-7405-ENG-48.

age ambient temperatures (cf. Fig. 3).

- A total daily draw of 0.278 m^3 (73 gal.) (cf. Fig. 3).

The system dimensions and the important parameters used in the DLM are presented in Table 1, and unless otherwise specified, pertain to all results.

RESULTS AND DISCUSSION

The DLM solves the governing equations of the system by using a finite-difference method. Numerical calculations are started at sunrise by specifying zero flow rate and by setting the system temperature equal to the ambient temperature at sunrise. The program is run for several days to obtain temperature and flow rate distributions. In Fig. 4 it is seen that at least three days are required to attain essentially steady-state performance for the case that includes a daily draw from the tank. The results presented in this study correspond to the steady-state condition (third day results) unless otherwise indicated.

Figure 5 is a plot of volumetric flow rate in the loop and energy transfer to the storage tank for the 24 hours of the third day. These plots correspond to no hot water draw from the storage tank, and therefore do not represent steady-state conditions. Flow rate curves are presented for three cases: an ordinary thermosiphon without heat exchanger using water as the circulating fluid, a thermosiphon with heat exchanger using water as the circulating fluid, and a thermosiphon with heat exchanger using p-glycol as the circulating fluid. For the two cases using water as the circulating fluid, the analytical results show night and early morning flow oscillations. While oscillations have been reported for non-solar natural convection systems [7-9], they have not been fully characterized for solar systems. However, experimental data from Baughn [10] and Shitzer et al. [11] have suggested the occurrence of the oscillations in solar thermosiphons. The cumulative energy transfers from the circulating fluids to the storage tanks, for the two heat exchanger cases (water and p-glycol), are also shown in Fig. 5. The deleterious effect of forward and reverse flow oscillations is shown by the nighttime decline of the cumulative energy transfer, for the case using water as the circulating fluid. The actual period of oscillations corresponds to the time required to fill both the riser and collector. Figure 5 does not show the actual period and magnitude of the oscillations, because the data is only plotted at half hour time intervals. Hence Fig. 5 indicates only the presence and approximate magnitude of the fluid oscillations when low viscosity fluids such as water are used. However, the cumulative energy transfer, from the circulating fluid to the storage tank, in Fig. 5 does indicate the actual effect of the fluid oscillations on the energy transfer. In contrast to the water behavior, p-glycol (which has higher viscosity) exhibits no oscillations, small reverse flow, and negligible nighttime energy losses. The analytical model thus indicates that there is a benefit from using p-glycol that tends to counteract the reductions in the system performance resulting from the incorporation of a heat exchanger.

An indication of the effect of the heat exchanger on system performance is given by Figs. 6(a) and 6(b). In Fig. 6(a) the 24-hour cumulative efficiency is plotted as a function of the variable HTR/(1+HTR), where HTR is the Heat Transfer Ratio, defined as $(UA)_{he}/(UA)_c$. Four points from DLM runs are used to generate each curve, which is then extrapolated to the line HTR/(1+HTR) = 1, in order to estimate the system performance for an ideal heat exchanger (infinite U_{he}). The maximum cumulative efficiency η_{max} thus determined is then used to produce the plots of normalized (third day) system efficiency versus HTR, shown in Fig. 6(b). Using a U_{he} of 170 W/m^2°C (30 Btu/hr°F-ft^2), three points are marked on the graph, corresponding to one, two, and three 2-inch heat exchanger tubes in parallel. These points are generated for very specific system parameters, use patterns, and climatic conditions, so restraint should be exercised in attempts to draw general conclusions. However, these results suggest that reasonable system performance can be achieved by a thermosiphon with a simple heat exchanger using p-glycol in the collector loop.

The effects of several parameters on the system performance are shown in Figs. 7-9. The tank temperature distribution is a complicated function of the energy delivery, the energy loss, and the mixing effect of supply water surges. In order to avoid modeling the details of the tank dynamics, a range of tank stratifications was selected, based on previous works on active systems. The sensitivity of system performance to tank stratification is shown in Fig. 7. The results indicate that tank stratification does not have a strong effect on the system performance.

The effects of tank elevation relative to the collector are shown in Fig. 8. The daytime flow rate decreases with decreasing tank elevation as a result of reduced buoyant forces. The reverse flow at night is negligible if the bottom of the tank is above or even with the top of the collector, but becomes substantial if the bottom of the tank is placed below the top of the collector. The deleterious effect of the reverse flow is apparent from the nighttime decline of the cumulative energy transfer which increases in severity with the rate of reverse flow. System performance is apparently not very sensitive to the daytime flow rate. The daytime energy transfer is the highest for the tank in the lowest position ($y = -1.22$ m). This result is attributable to the lower system temperatures which result from the nighttime reverse-flow losses.

The effects of flow resistance are shown in Figs. 9(a) and 9(b). Figure 9(a) tends to confirm the previous results, which showed that over a large range, a decrease in the flow rate has a small effect on system performance. The energy transfers are indistinguishable for collector tube sizes greater than or equal to the nominal 1/4 in. diameter (I.D. = 0.315 in. = 0.800 cm). Collector tubes of nominal 1/8 in. diameter (I.D. = 0.190 in. = 0.483 cm) produce a slight reduction in system performance. Figure 9(b) shows the effects of connecting pipe diameter for a total connecting pipe length of 8.4 m (27.5 ft). These results tend to confirm the previous studies of non-heat exchanger systems that show the "self compensating" nature of buoyancy-driven flows [2,4].

As mentioned before, all results presented apply only to an average June day in Richmond, Ca. While these results indicate the system potential, they should not be generalized. The following studies are necessary to fully establish the technical and economic viability of this type of freeze protected thermosiphon water heater:

- Experimental validation of the Detailed Loop Model (DLM).
- Development of a simplified, Correlative Analysis Tool (CAT) to study the annual performance of thermosiphons with heat exchangers in various climates.
- Comparison of the performances of vertical and horizontal tanks.
- Designing of heat exchangers for thermosiphon systems with vertical and horizontal tanks.

CONCLUSIONS

Several preliminary conclusions are deduced from the DLM studies:

- Reasonable system performance can be achieved by a thermosiphon with a simple heat exchanger, using p-glycol as the circulating fluid.
- Night oscillations and reverse flow are suppressed when p-glycol is used as a circulating fluid and the bottom of the tank is not below the top of the collector.
- No significant performance advantage results from elevating the bottom of the tank above the top of the collector (i.e., above the limiting point necessary to suppress the reverse flow).
- System performance is essentially independent of flow resistance over a wide range of resistance values.
- System performance is sufficiently insensitive to tank stratification that reasonably accurate calculations can be made based on empirical estimates of the stratification.

NOMENCLATURE

A	surface area, m^2 (ft^2)
c	specific heat, kJ/kg^oC (Btu/lbm^oF)
d	diameter, cm (in.)
E_t	cumulative energy transfer to storage tank, kcal (Btu)
F'	plate efficiency factor
HTR	heat transfer ratio = $(UA)_{he}/(UA)_c$
L	length, m (ft)
L_t	total connecting pipe length, m (ft)
M	total number of heat exchanger tubes
N	total number of collector tubes
q	heat flux, W/m^2 (Btu/hr-ft^2)
Q	volumetric flow rate, m^3/sec (gal/min)
S_t	daily total solar radiation, kcal/m^2day (Btu/ft^2day)
T	temperature, ^oC (^oF)
ΔT	temperature difference between top and bottom of storage tank, ^oC (^oF)
U	overall heat transfer coefficient, W/m^2 ^oC (Btu/hr-ft^2 ^oF)
U_L	overall collector loss coefficient, W/m^2 ^oC (Btu/hr-ft^2 ^oF)
V	total volume of storage tank, m^3 (gal)
$\mathring{V}$	amount of draw, m^3/day (gal/day)

y	vertical position of tank bottom relative to collector top, m (ft)
α	normal absorptivity of collector absorber plate
β	thermal expansion coefficient, $1/^{o}K$ $(1/^{o}R)$
η	cumulative efficiency
θ	collector tilt angle
μ	absolute viscosity, cp (lbm/ft-hr)
ρ	density, kg/m^3 (lbm/ft^3)
τ	normal transmissivity of the collector cover plate

Subscripts

a	ambient
c	collector
cp	connecting pipes
h	header
he	heat exchanger
in	insulation
max	maximum
s	supply
sr	solar radiation
tk	storage tank

TABLE 1. SYSTEM DIMENSIONS AND PARAMETERS*

A_c = 2×1.95 (2×21)	N = 2×9
d_c = 0.953 (0.375)	S_t = 4803.5 (1766)
d_{cp} = 2.604 (1.025)	T_s = 16.7 (62)
d_h = 2.680 (1.055)	ΔT = 5.5 (10)
d_{he} = 5.042 (1.985)	$U_c = F'U_L$ = 4.201 (0.741)
d_{tk} = 50.8 (20)	U_{he} = 170.1 (30)
F' = 0.9	U_{in} = 0.85 (0.15)
L_c = 1.75 (5.75)	V = 0.302 (80)
L_h = 4×1.12 (4×3.67)	$\dot{V}$ = 0.278 (73)
L_{he} = 1.52 (5)	θ = 45
L_t = 4.54 (14.9)	$\tau\alpha$ = 0.86
L_{tk} = 1.52 (5)	No. of elbows = 10
M = 3	No. of tees = 4
CLIMATE: Richmond, Ca. in June	
Heat transfer fluid is 60% p-glycol by weight	

*Units are given in the Nomenclature

REFERENCES

[1] Fanney, A.H. and Liu, S.T., "Comparison of Experimental and Computer Predicted Performance for Six Solar Domestic Hot Water Systems," ASHRAE Symposium on Solar Hot Water Systems, Los Angeles, Ca., February 1980.

[2] Close, D.J., "The Performance of Solar Water Heater With Natural Circulation," Solar Energy, 6, 33-40 (1962).

[3] Bergquam, J.B., Young, M.F., Perry, S., and Baughn, J.W., "A Comparative Study of SDHW Systems in California," Report to the California Energy Commission (June 1979).

[4] Place, W., Daneshyar, M. and Kammerud, R., "Mean Monthly Performance of Passive Solar Water Heaters," in Proceedings, 4th Nat'l Passive Solar Conf., Kansas City, Mo., 3-5 October 1979, 4, 601-604 (Lawrence Berkeley Laboratory Report LBL-9195).

[5] American National Standard, "Solar Heat Exchangers," ANSI/ASME SES 1, May 1979 (Draft).

[6] Mertol, A., Place, W., Webster, T., and Greif, R., "Detailed Loop Model (DLM) Analysis of Liquid Solar Thermosiphons With Heat-Exchangers," Lawrence Berkeley Laboratory Report LBL-10699 (1980).

[7] Zvirin Y., Jeuck III, P.R., Sullivan, C.C. and Duffey, R.B., "Experimental and Analytical Investigation of a PWR Natural Circulation Loop," ANS/ENS Thermal Reactor Safety Meeting, Knoxville, Tenn., April 1980.

[8] Greif, R., Zvirin, Y. and Mertol, A., "The Transient and Stability Behavior of a Natural Convection Loop," J. Heat Transfer, 101, 684-688 (1979).

[9] Mertol, A., "Heat Transfer and Fluid Flow in Thermosiphons," Ph.D. Thesis, University of California, Berkeley (1980).

[10] Baughn, J.W., University of California, Davis (private communications).

[11] Shitzer, A., Kalmanoviz, D., Zvirin, Y., and Grossman, G., "Experiments With a Flat Plate Solar Water Heating System In Thermosyphonic Flow," Solar Energy, 22, 27-35 (1979).

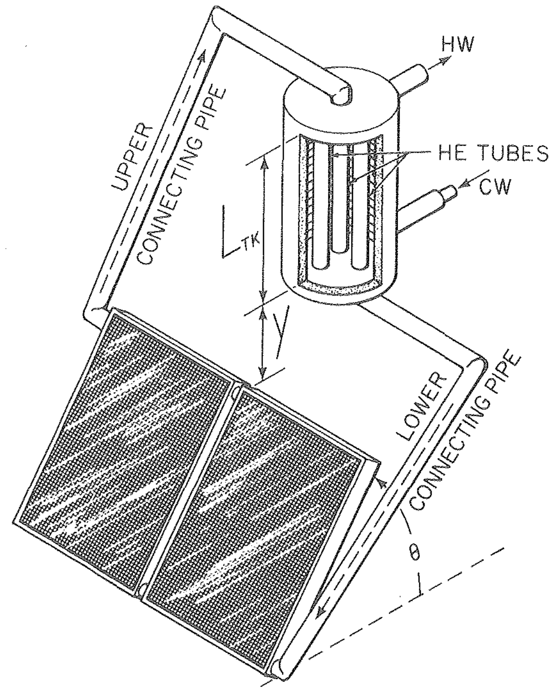

FIG. 1 Thermosiphon water heater

XBL 803-6909

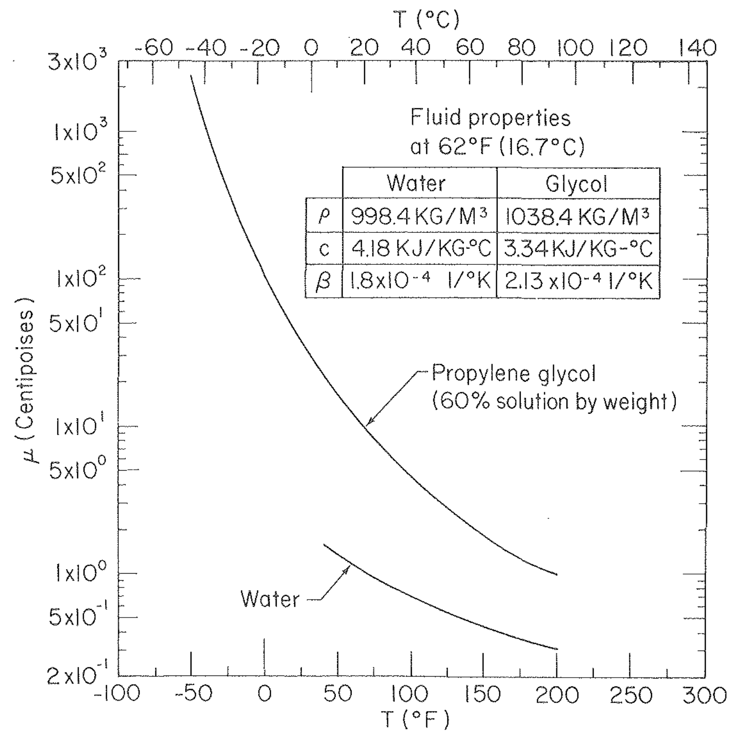

	Water	Glycol
ρ	998.4 KG/M³	1038.4 KG/M³
c	4.18 KJ/KG-°C	3.34 KJ/KG-°C
β	1.8×10^{-4} 1/°K	2.13×10^{-4} 1/°K

FIG. 2 Fluid properties

XBL 805-6993

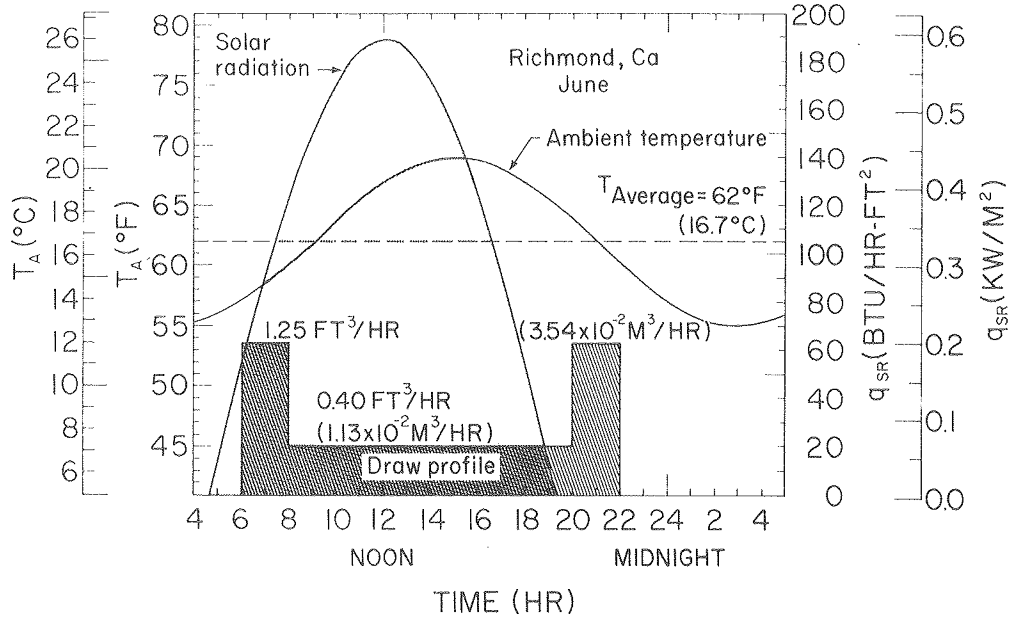

FIG. 3 Design day data

XBL 803-6903

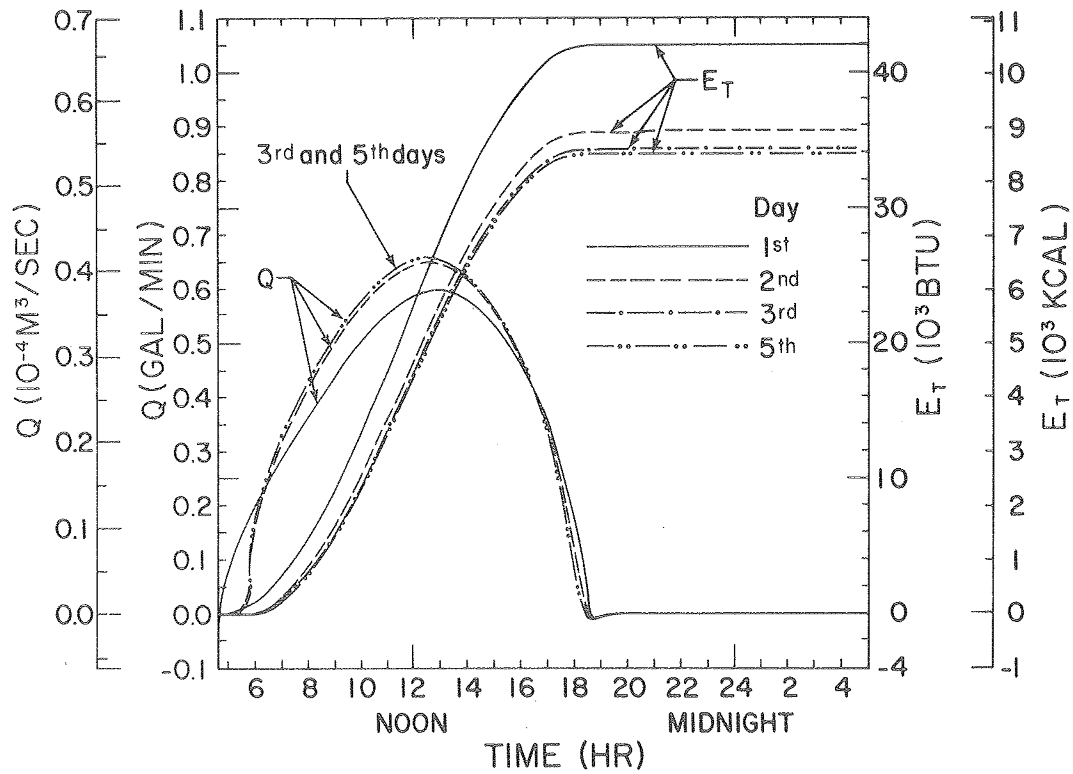

FIG. 4 Initialization of DLM

XBL 803-6906

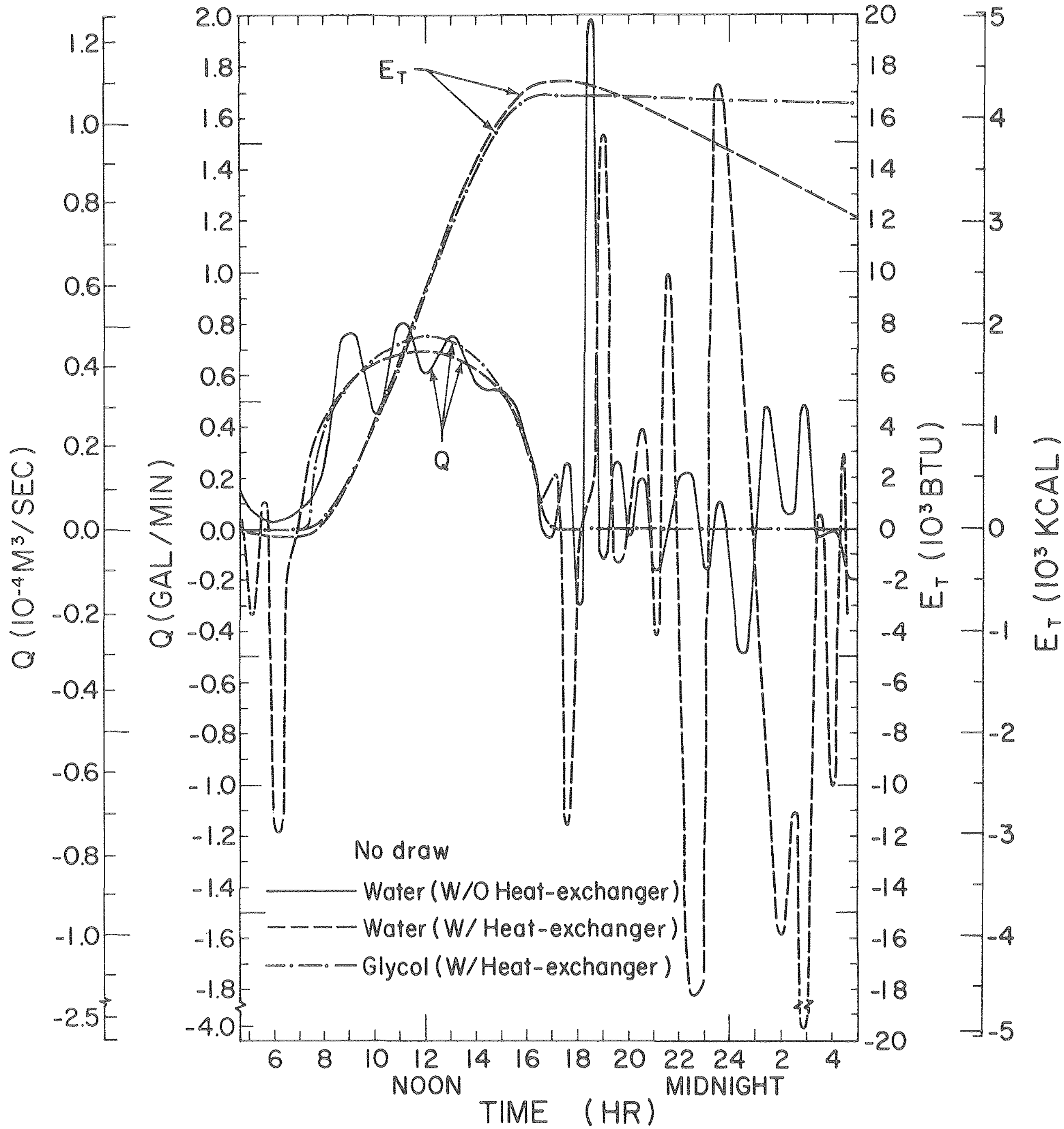

FIG. 5 Examples of fluid oscillations and their effects on system performance

XBL 803-6902

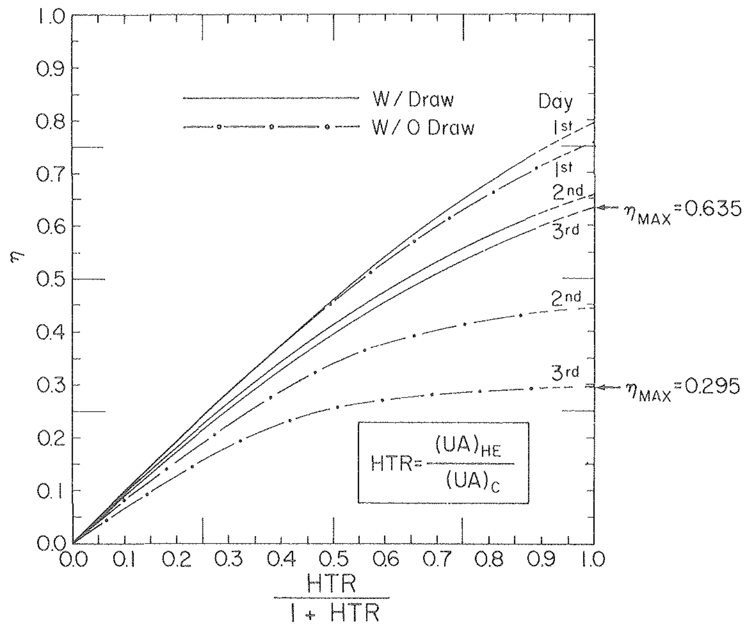

FIG. 6 (a) Effect of HTR on cumulative system efficiency

XBL 803-6905

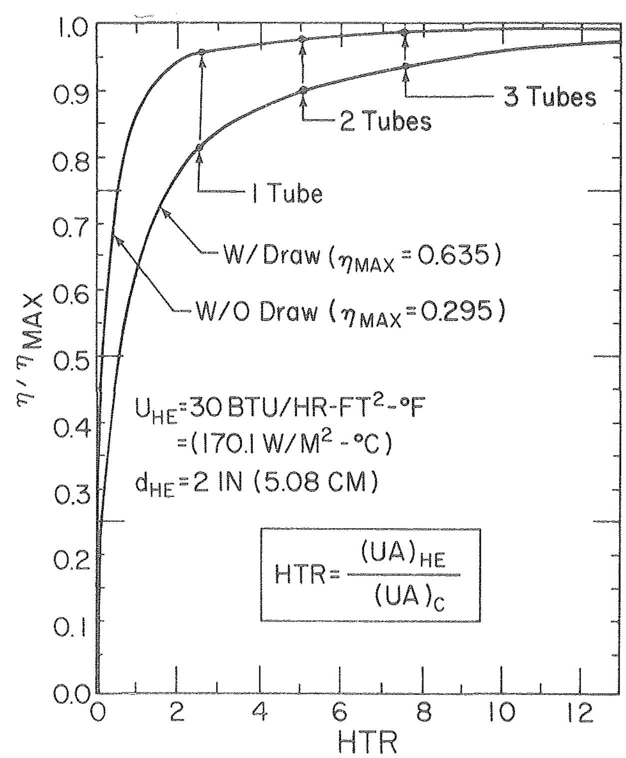

FIG.6(b) Effect of HTR on normalized system efficiency

XBL 803-6904

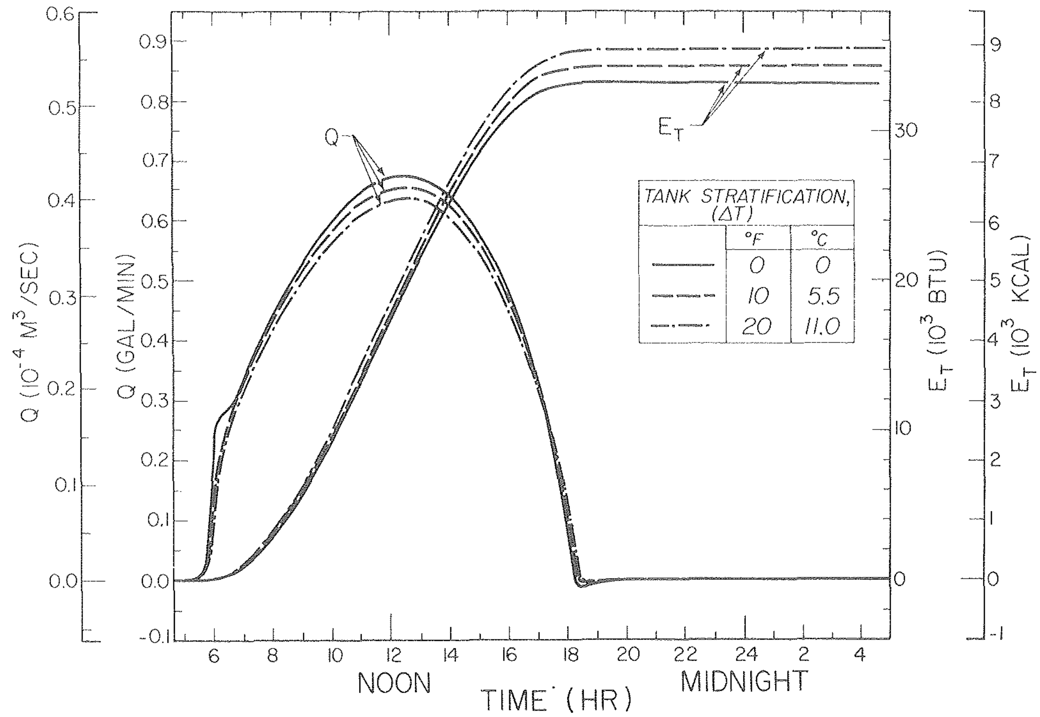

FIG. 7 Effect of tank stratification

XBL 803-523

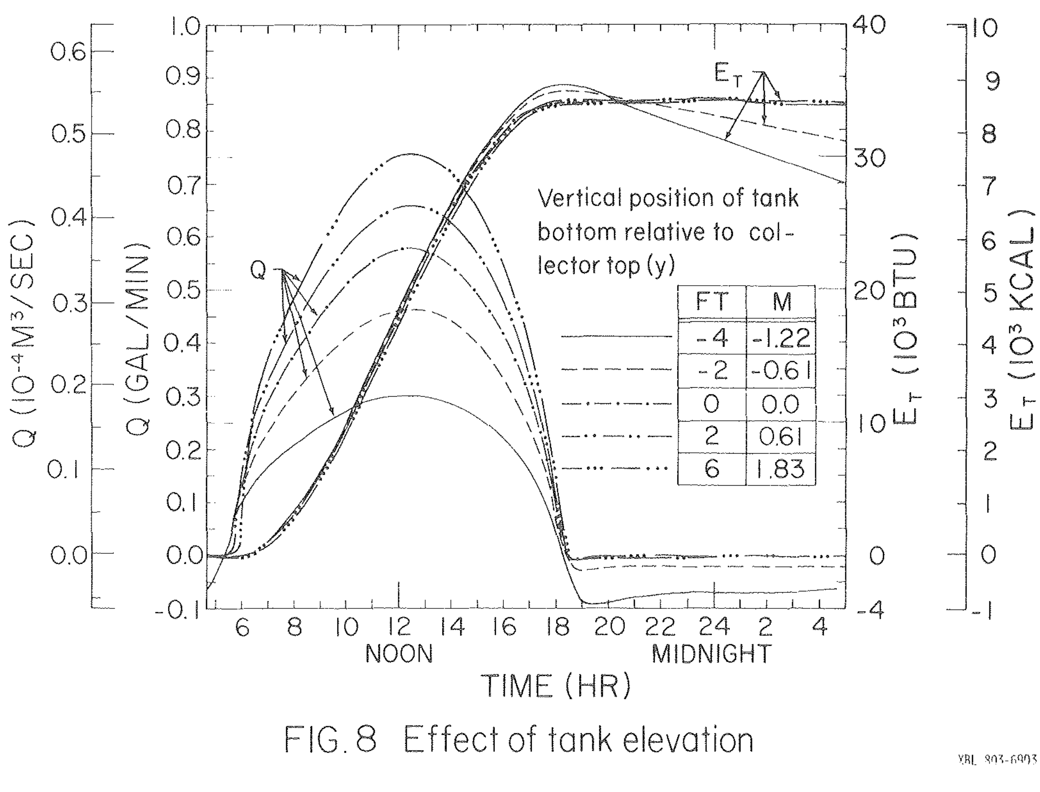

FIG. 8 Effect of tank elevation

XBL 803-6993

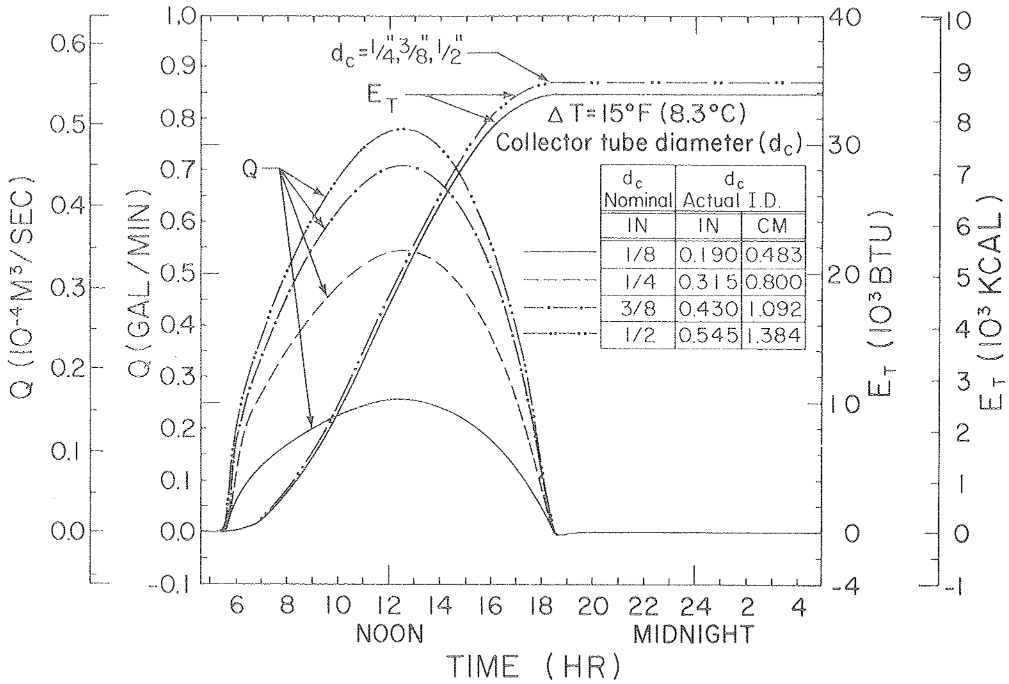

FIG. 9(a) Effect of collector tube diameter

XBL 803-6997

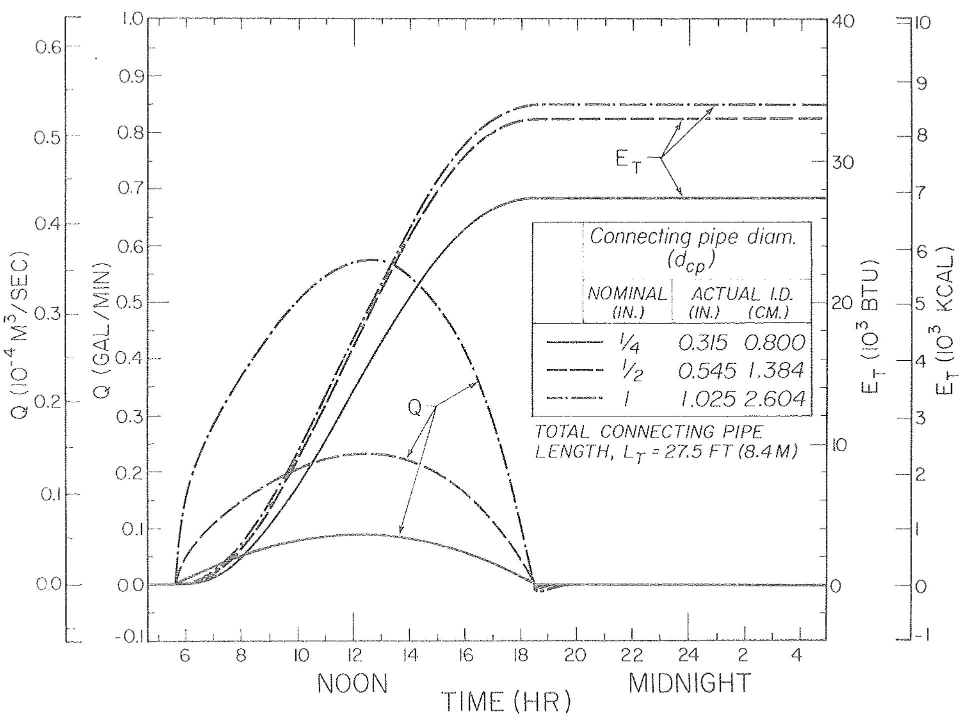

FIG. 9(b) Effect of connecting pipe diameter XBL 803-522